

Possible undercompensation effect in the Kondo insulator (Yb,Tm)B₁₂P. A. Alekseev,^{1,2} K. S. Nemkovski,³ J.-M. Mignot,⁴ E. S. Clementyev,^{1,2,5} A. S. Ivanov,⁶ S. Rols,⁶ R. I. Bewley,⁷ V. B. Filipov,⁸ and N. Yu. Shitsevalova⁸¹National Research Centre ‘Kurchatov Institute,’ 123182 Moscow, Russia²National Research Nuclear University ‘MEPhI,’ 115409, Moscow, Russia³Jülich Centre for Neutron Science JCNS, Forschungszentrum Jülich GmbH, Outstation at MLZ, Lichtenbergstraße 1, 85747 Garching, Germany⁴Laboratoire Léon Brillouin, CEA-CNRS, CEA/Saclay, 91191 Gif sur Yvette, France⁵Institute for Nuclear Research RAS, Troitsk, MR, Russia⁶Institut Laue-Langevin, BP 156, 38042 Grenoble Cedex 9, France⁷ISIS Pulsed Neutron and Muon Facility, Rutherford Appleton Laboratory, Chilton, Didcot OX11 0QX, United Kingdom⁸I. N. Frantsevich Institute for Problems of Materials Science, 03142 Kiev, Ukraine

(Received 7 November 2013; published 20 March 2014)

The effects of Tm substitution on the dynamical magnetic response of Yb_{1-x}Tm_xB₁₂ ($x = 0, 0.08, 0.15$, and 0.75) and Lu_{0.92}Tm_{0.08}B₁₂ compounds have been studied using time-of-flight inelastic neutron scattering. Major changes were observed in the spectral structure and temperature evolution of the Yb contribution to the inelastic response for a rather low content of magnetic Tm ions. A sizable influence of the RB₁₂ host (YbB₁₂, as compared to LuB₁₂ or pure TmB₁₂) on the crystal-field splitting of the Tm³⁺ ion is also reported. The results point to a specific effect of impurities carrying a magnetic moment (Tm, as compared to Lu or Zr) in a Kondo insulator, which is thought to reflect the “undercompensation” of Yb magnetic moments, originally Kondo screened in pure YbB₁₂. A parallel is made with the strong effect of Tm substitution on the temperature dependence of the Seebeck coefficient in Yb_{1-x}Tm_xB₁₂, which was reported previously.

DOI: [10.1103/PhysRevB.89.115121](https://doi.org/10.1103/PhysRevB.89.115121)

PACS number(s): 75.20.Hr, 75.30.Mb, 78.70.Nx

I. INTRODUCTION

Among strongly correlated electron systems, Kondo insulators are considered promising candidates for the design of high-performance low-temperature thermoelectric materials because of their rather high Seebeck thermoelectric power coefficient (TEP) coefficients (hundreds of microvolts per Kelvin) [1]. Recently a new series of Yb_{1-x}Tm_xB₁₂ solid solutions, based on the archetype Kondo insulator YbB₁₂, has been prepared [2]. It was shown that partial substitution of Yb by Tm ions results in a considerable enhancement of the thermoelectric power [2] in the temperature range 15–150 K, whereas no such effect is observed in the case of Lu substitution [3] (Fig. 1). Lu is isovalent to Tm but carries no magnetic moment owing to its filled *f*-electron shell. Therefore, the thermoelectric enhancement has to be somehow related to the magnetic moments of the substituent ions. Theoretical models or *ab initio* simulations are unfortunately not yet able to provide a quantitative description of these properties, even for undoped YbB₁₂. On the other hand, the microscopic behavior of the magnetic subsystem can be directly addressed by means of inelastic neutron scattering experiments.

The ground state of YbB₁₂ is a nonmagnetic singlet with dynamical antiferromagnetic correlations [4]. It transforms to a single-site spin-fluctuation regime above 60 K, with a characteristic spin-fluctuation temperature T_{sf} on the order of 100 K. The low-temperature regime is characterized by the existence of both a charge [5] and a spin [6] gap. In addition, a resonance mode (RM) of spin-exciton type with sizable dispersion was shown to exist at about 15 meV, below the spin-gap edge, for temperatures lower than about 40 K [7,8]. A cooperative state thus appears to form in this temperature range as a result of Kondo-like compensation effects in the strongly correlated electron system.

The substitution of Tm³⁺ ions on the Yb lattice provides randomly distributed unscreened magnetic moments, which can strongly disturb the cooperative Kondo-lattice state. To the best of our knowledge, the study of such effects in Kondo insulators was limited so far to thermodynamic or transport measurements [9]. In the case of the (Yb,Tm)B₁₂ series, the substitution is isovalent and does not disturb the crystal lattice nor the band structure significantly. Furthermore, the lattice constants of YbB₁₂ (7.4690 Å) and TmB₁₂ (7.4675 Å) [10] are very close and no chemical pressure effect is thus expected. The Tm ions introduced on the rare-earth (RE) sublattice can thus be regarded as pure “magnetic moment defects” (a triplet crystal-field ground state is expected for Tm³⁺ [11]).

Inelastic magnetic scattering of a thermal neutron is the probe of choice for analyzing the composition and temperature dependences of the dynamical magnetic susceptibility. The paper presents new experimental results obtained in a wide range of temperatures. They provide evidence of the dramatic effect of Tm magnetic moments on the shape and temperature evolution of the gapped magnetic excitation spectrum in YbB₁₂. The spin gap transforms to a quasigap for only 15% Tm substitution, and the spin-exciton resonance mode is suppressed at even lower concentrations. We also point out possible connections between this evolution of the microscopic magnetic state and the strong transformation observed in the thermoelectric properties.

II. EXPERIMENTAL DETAILS**A. Sample preparation**

Solid solutions of the Yb_{1-x}Tm_xB₁₂ ($x \equiv x_{Tm} = 0.75, 0.15, 0.08$) have been synthesized at the Institute of Problems of Materials in Kiev by borothermal reduction from a mixture

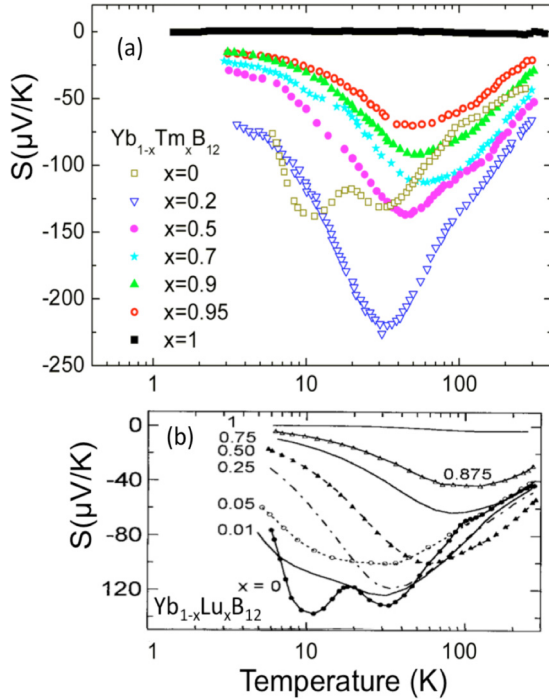


FIG. 1. (Color online) Thermoelectric power of (a) $\text{Yb}_{1-x}\text{Tm}_x\text{B}_{12}$ [2] and (b) $\text{Yb}_{1-x}\text{Lu}_x\text{B}_{12}$ [3] as a function of temperature. Data for YbB_{12} in both frames are taken from Ref. [3].

of ytterbium and thulium oxides performed under vacuum at 1700 °C. ^{11}B isotope (99.5% or 99.3% enrichment) was used in order to reduce neutron absorption. The materials were subsequently remelted under Ar pressure using the traveling-solvent floating-zone technique. For $x = 0.15$ and 0.75, single crystals of satisfactory quality (few grains with a mosaic spread of 2.5 deg) with masses of a few grams could be grown by this method. In some cases, after checking by x rays, the samples were powdered and etched with nitric acid to remove the YbB_6 phase. X-ray diffraction measurements confirmed all compounds to have the fcc structure with the expected lattice parameter.

A $\text{Lu}_{0.92}\text{Tm}_{0.08}\text{B}_{12}$ sample was also prepared using the same method. In order to single out the influence of Tm ions on the original magnetic signal from Yb, a quantitatively reliable procedure is needed for subtracting the Tm contribution from total magnetic scattering intensity. This task is complicated by the strong neutron magnetic scattering cross section of Tm^{3+} , larger by about a factor of 3 than that of Yb^{3+} , and by the qualitative difference between their respective spectral shapes (narrow peaks for Tm and distributed for Yb). A direct measurement of the Tm contribution in a magnetically “inert” reference compound is therefore required.

Measurements of YbB_{12} and LuB_{12} samples from previous studies [6] were repeated in the present experiments, mainly to allow comparisons between Tm-substituted and unsubstituted compounds to be performed on spectra obtained under identical conditions. Pure LuB_{12} also served as a reference for subtracting phonon contributions when data could not be collected at sufficiently large momentum transfers ($\geq 7 \text{ \AA}^{-1}$).

B. Experimental conditions

A first series of neutron measurements was performed on the thermal-neutron time-of-flight spectrometer MERLIN at ISIS (RAL). This machine has a moderate resolution and a detector array covering a large solid angle, which allows collective effects to be studied using single crystals. In this experiment we have investigated the spin dynamics in $\text{Yb}_{1-x}\text{Tm}_x\text{B}_{12}$ ($x_{\text{Tm}} = 0.15, 0.75$) over a wide energy range, using incident neutrons of energy $E_i = 80 \text{ meV}$ (resolution $\Delta E = 5 \text{ meV}$ at zero energy transfer). The samples were *single crystals* with masses of 2.78 and 9.33 g, respectively (for $x_{\text{Tm}} = 0.75$ the sample actually consisted of two separate pieces). A LuB_{12} *powder* specimen was used to estimate the nonmagnetic contribution to the measured spectra.

The measurements were carried out at $T = 6, 75, 150,$ and 250 K for $x_{\text{Tm}} = 0.15$ by rotating the crystal around the vertical axis in order to collect the whole four-dimensional momentum-energy map. For $x_{\text{Tm}} = 0.75$, cooperative effects are expected to be less pronounced, owing to the lower Yb content, and the corresponding spectra were thus recorded only for one fixed sample rotation angle at two temperatures, $T = 7$ and 150 K .

To get more detailed information in the low-energy range (quasielastic region and near the spin-gap edge), we performed extensive measurements on the IN4C time-of flight spectrometer at the ILL. Only powder samples with $x_{\text{Tm}} = 0, 0.08,$ and 0.15 were used in that experiment. The incoming energy was $E_i = 36 \text{ meV}$, giving an energy resolution $\Delta E = 1.75 \text{ meV}$ (pyrolytic graphite PG[002] monochromator) at zero energy transfer. Measurements were done in the temperature range $2 < T < 80 \text{ K}$.

The powdered samples were enclosed in flat sachets folded from $28 \mu\text{m}$ thick Al foil, with a total area of $40 \times 20 \text{ mm}^2$ and a controlled thickness of 2 mm. The total mass of powder was around 4 g for each sample, and the total amount of Al in the beam was less than 0.5 g, guaranteeing a low level of contamination by Al scattering. Separate measurements of the empty Al container and of a vanadium standard were used to correct the experimental spectra from the nuclear background and for detector calibration.

Because of the relatively low energy of incident neutrons on IN4C, the momentum transfer achieved for the largest accessible scattering angle was not sufficient to fully suppress the magnetic signal. The phonon background thus had to be determined indirectly from the corresponding LuB_{12} spectra (see below). The uncertainty in extracting the magnetic signal was further reduced by restricting the data treatment to detector groups with low scattering angles, from $2\Theta = 13^\circ$ to 32° ($\langle 2\Theta \rangle = 22^\circ$), for which the relative weight of phonon scattering is weakest.

After background subtraction and application of instrumental corrections (empty can contribution), the spectra were remapped on a linear energy scale and normalized to a fixed number of RB_{12} formula units. Energy dependent transmission corrections for each sample were also applied. The transmission coefficient at zero energy transfer was within the limits of 0.70 to 0.75 for all samples measured.

III. RESULTS

A. Wide energy range (MERLIN)

In the single-crystal measurements we expected to observe some extra magnetic scattering near the L point, $\mathbf{q} = (1/2, 1/2, 1/2)$, reminiscent of the resonance mode previously observed in YbB_{12} [4,7]. This expectation, however, was not fulfilled, even for the compound with the lower Tm content ($x_{\text{Tm}} = 0.15$). The experimental observation is that no emergence of an extra signal, besides the contribution from Tm, could be detected close to the L point at low momentum transfer ($|\mathbf{Q}| \sim 1 \text{ \AA}^{-1}$) with decreasing temperature.

A preliminary analysis was thus done by averaging the spectra over all sample rotation angles and treating the result as polycrystal data [12]. The phonon contribution was then subtracted using the standard procedure for polycrystalline samples [13]. The obtained *magnetic* spectra are shown in Fig. 2. From this plot one sees that the Tm crystal-field (CF) contribution (total magnetic cross section $\sigma_{\text{mag}} = 35 \text{ b}$) dominates in the spectra for $\text{Yb}_{0.25}\text{Tm}_{0.75}\text{B}_{12}$ (b), and still seems to give a sizable contribution in the case of $\text{Yb}_{0.85}\text{Tm}_{0.15}\text{B}_{12}$ (a). However, the most intense peaks are located at $E_1 \approx 7.5 \text{ meV}$ and $E_2 \approx 14 \text{ meV}$, and the upper transition energy E_3 does not exceed 30 meV , in agreement with the results obtained for TmB_{12} [11]. The magnetic signal above this limit thus arises from Yb alone and can be treated unambiguously.

At low temperature, both samples exhibit a pronounced broad peak at an energy of about 40 meV , similar to that previously reported for undoped YbB_{12} [6]. In the latter compound, the peak was suppressed by increasing temperature to 60 K , giving place to a broad quasielastic signal. A similar effect seems to occur in $\text{Yb}_{0.85}\text{Tm}_{0.15}\text{B}_{12}$ [Fig. 2(a)]. For $\text{Yb}_{0.25}\text{Tm}_{0.75}\text{B}_{12}$ [Fig. 2(b)], on the other hand, the temperature

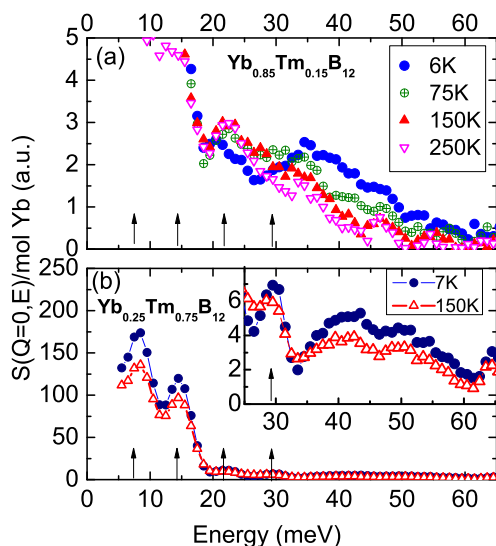


FIG. 2. (Color online) Magnetic spectral response of (a) $\text{Yb}_{0.85}\text{Tm}_{0.15}\text{B}_{12}$ and (b) $\text{Yb}_{0.25}\text{Tm}_{0.75}\text{B}_{12}$ measured on MERLIN (ISIS) with incident neutron energy $E_0 = 80 \text{ meV}$ and energy resolution $\Delta E_0 = 5 \text{ meV}$ at different temperatures, reduced to $Q = 0$ according to the Tm^{3+} form factor. Arrows indicate the positions of the thulium CF excitations defined for TmB_{12} at low temperature [9]. Inset in frame (b) same data plotted on an expanded scale.

evolution appears to be dominated by the effect of the detailed-balance factor for Tm-originated excitations in the region below 30 meV and perhaps for Yb-originated signal at higher energies.

To summarize this part, the general structure of the Yb magnetic excitation spectra above the energy range of Tm-related excitations seems to be similar to that observed in undoped YbB_{12} , despite the fact that no clear evidence of the dispersive RM-like excitation around L point could be found in the present single-crystal study. Possible changes due to Tm substitution have to be searched for in the low energy transfer range. It is thus worthwhile to focus on the study of spin gap and near-edge region with increased resolution. Single-crystal measurements, on the other hand, may not be critical at this stage, especially if one recalls that, for pure YbB_{12} , the near-edge structure, and in particular the RM, were clearly identified in the powder experiments.

B. Spin-gap energy range (IN4C)

In this part of the work, a major experimental issue was the separation of the magnetic spectral response due to Yb from that due to the Tm CF transitions, which clearly dominates the inelastic neutron spectra. To this purpose, we have measured not only $\text{Yb}_{1-x}\text{Tm}_x\text{B}_{12}$ compounds with three different concentrations $x_{\text{Tm}} = 0, 0.08, \text{ and } 0.15$, but also one $\text{Lu}_{0.92}\text{Tm}_{0.08}\text{B}_{12}$ and one pure LuB_{12} sample, in order to determine the experimental magnetic signal from Tm under identical experimental conditions (same instrument, incident energy, energy resolution, etc.). The results of the measurements on LuB_{12} and $\text{Lu}_{0.92}\text{Tm}_{0.08}\text{B}_{12}$ at 2 K are shown in Fig. 3, along with a fit of the phonon (for LuB_{12} solid

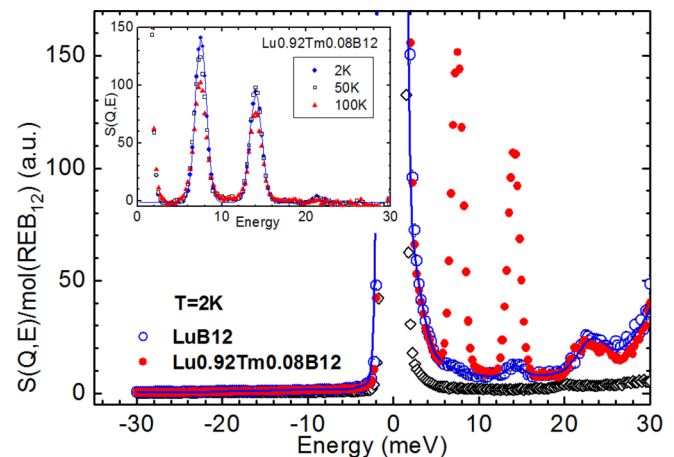


FIG. 3. (Color online) Spectra obtained on IN4C (ILL) at incident neutron energy $E_0 = 36 \text{ meV}$ and scattering angle $(2\Theta) = 22^\circ$ for LuB_{12} (open circles) and $\text{Lu}_{0.92}\text{Tm}_{0.08}\text{B}_{12}$ (closed circles) measured at $T = 2 \text{ K}$; a vanadium spectrum ($T \sim 100 \text{ K}$) is shown by open diamonds; the solid line denotes the fit to the LuB_{12} spectrum, representing the phonon contribution to the scattering function. Inset: magnetic component of the $\text{Lu}_{0.92}\text{Tm}_{0.08}\text{B}_{12}$ spectra at $2, 50, \text{ and } 100 \text{ K}$ (dots, open squares, triangles, respectively), associated with the Tm^{3+} CF excitations, after subtraction of the phonon contribution; the line is a fit to the spectrum at $T = 2 \text{ K}$ by Gaussian line shapes.

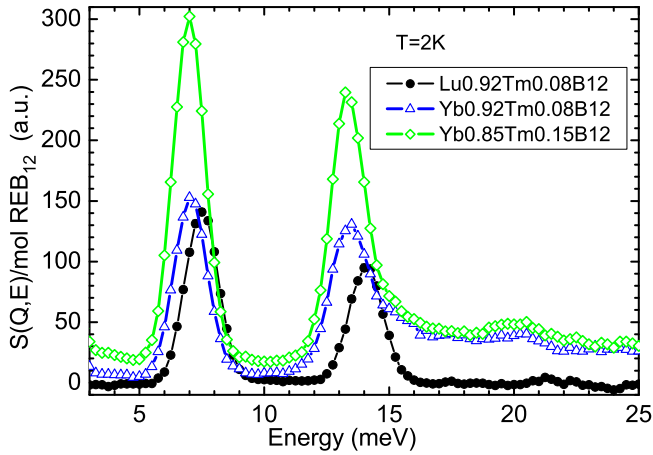


FIG. 4. (Color online) Magnetic scattering spectra (phonons subtracted) of $\text{Yb}_{0.92}\text{Tm}_{0.08}\text{B}_{12}$ (triangles) and $\text{Yb}_{0.85}\text{Tm}_{0.15}\text{B}_{12}$ (diamonds) in comparison with that of $\text{Lu}_{0.92}\text{Tm}_{0.08}$ (dots) at $T = 2$ K. Measurements performed on IN4C (ILL), at incident energy $E_0 = 36$ meV (energy resolution $\Delta E_0 = 1.75$ meV).

line in the main frame) and magnetic (for $\text{Lu}_{0.92}\text{Tm}_{0.08}\text{B}_{12}$ solid line in the inset) components. The temperature dependence of the magnetic signal is shown in the inset for the range between 2 and 80 K. One clearly distinguishes three transitions between CF levels, in good correspondence with the only results reported so far for pure TmB_{12} [11], and there is no significant shift or broadening of the CF peaks in the temperature range studied. It can be noted that the strongest two CF excitations for Tm^{3+} occur, respectively, deep within the spin gap (≈ 7 meV) and close to the energy (≈ 14 meV) of the first peak in the phonon density of states, as well as to that of the RM in the magnetic response of YbB_{12} .

The phonon contribution to the $\text{Yb}_{1-x}\text{Tm}_x\text{B}_{12}$ spectra was calculated from the LuB_{12} spectra measured at temperatures from 2 to 100 K. It is well established, from a previous lattice dynamics study [14], that the RE nuclear scattering cross section is responsible for the phonon peak at 15 meV in the phonon density of states of YbB_{12} . In the incoherent approximation, the intensity of this peak reflects the total scattering cross section of the RE ion. Therefore, the scaling factor corresponding to the ratio of the total RE cross sections ($\sigma_{\text{tot}}[\text{Lu}:\text{Tm}:\text{Yb}] = 1.0.9.3.25$) was applied only to the amplitude of the 15 meV phonon peak in the smoothed scattering function of LuB_{12} , in order to reconstruct a spectrum representing the estimated phonon contribution in $\text{Yb}_{1-x}\text{Tm}_x\text{B}_{12}$.

Figure 4 shows the magnetic components in $\text{Lu}_{0.92}\text{Tm}_{0.08}\text{B}_{12}$ and $\text{Yb}_{1-x}\text{Tm}_x\text{B}_{12}$ for $T = 2$ K. Unexpectedly, a systematic shift of the Tm^{3+} CF peaks is observed between the Lu- and Yb-based compounds. Furthermore, the amplitude of this shift increases almost linearly with the excitation energy, according to a fit of the first two (strongest) peaks, with a relative shift $\Delta E/E$, averaged over the three main peaks, of about 4%. It also appears to be independent of the Tm concentration and of the measuring temperature, at least up to 80 K, which is the range of interest

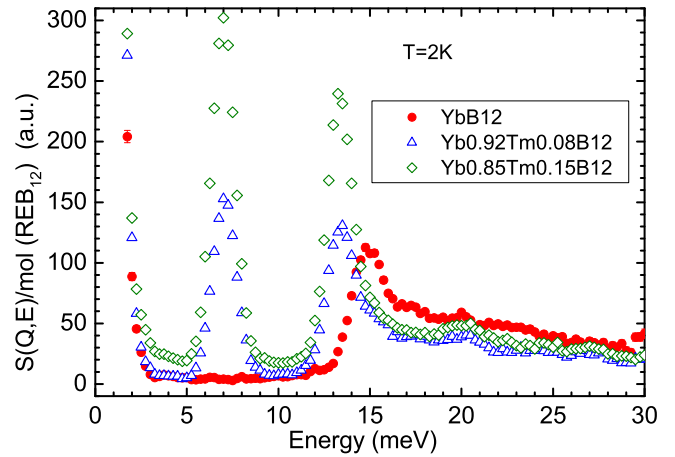


FIG. 5. (Color online) Magnetic scattering spectra of $\text{Yb}_{1-x}\text{Tm}_x\text{B}_{12}$ at $T = 2$ K (same data and markers as in Fig. 4) compared with the magnetic spectrum for YbB_{12} (closed circles) measured under the same conditions.

here.¹ In these materials the Tm^{3+} ions serve as a probe of the intrinsic CF potential in the LuB_{12} or YbB_{12} matrix, and clearly feel the difference between the two.

In Fig. 5 the magnetic scattering component at $T = 2$ K is presented for pure YbB_{12} and the two $\text{Yb}_{1-x}\text{Tm}_x\text{B}_{12}$ solid solutions. The spectra basically consist of strong, resolution-limited, CF excitations from Tm^{3+} , superimposed on a wide gapped spectrum similar to that of YbB_{12} . To separate out the signal from Yb, one must subtract the (strong) Tm CF excitations and the (much weaker) phonon background.

The results, normalized to the number of Yb ions, are presented in Figs. 6(a)–6(c) for $x_{\text{Tm}} = 0, 0.08, \text{ and } 0.15$. Several observations can be made from these plots. The first one is that, in YbB_{12} , the narrow peak associated with the RM at 15 meV is already strongly suppressed when temperature is raised to no more than 30 K, i.e., just before the spin gap begins to fill. This is in good agreement with our recent single-crystal data [8], which demonstrated the complete suppression of the RM at $\mathbf{q} = (1/2, 1/2, 1/2)$ above 40 K, without a significant shift in its energy [Figs. 7(a) and 7(b)]. It also confirms a previous study of the temperature evolution of the magnetic spectral response in YbB_{12} powder [8, 15], which concluded to a filling of the gap by a quasielastic signal [Fig. 7(c)].

In Figs. 6(b) and 6(c)² the spectra exhibit some residual structure near 15 meV. However, its intensity represents less than 10% of that of the RM peak in pure YbB_{12} , as shown in Fig. 6(a). Furthermore, the effect appears more pronounced in the compound with the larger Tm concentration, which is clearly unphysical. It could result from uncertainties in subtracting out the phonon background, or in separating the Yb magnetic signal from the strong Tm CF excitations. However, if one estimates the magnitude of this latter effect from the

¹Above this temperature the Yb magnetic response is almost completely transformed from gaplike to spin-fluctuation-like (see Introduction).

²See also Figs. 8(c) and 8(d) below.

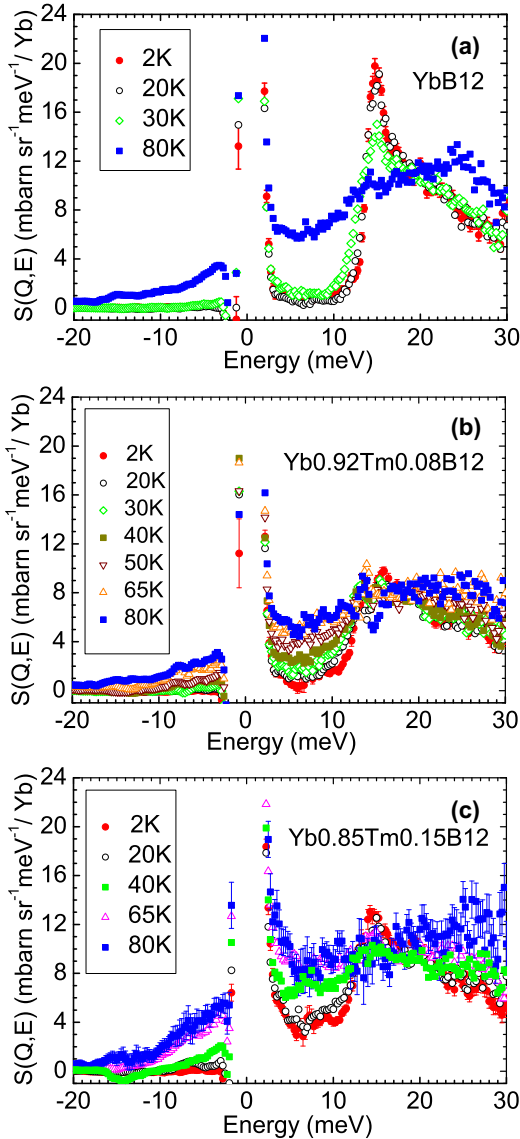


FIG. 6. (Color online) Yb contribution to the magnetic scattering spectra for $\text{Yb}_{1-x}\text{Tm}_x\text{B}_{12}$, obtained by subtracting phonon scattering and the Tm contribution (a) YbB_{12} , (b) $\text{Yb}_{0.92}\text{Tm}_{0.08}\text{B}_{12}$, and (c) $\text{Yb}_{0.85}\text{Tm}_{0.15}\text{B}_{12}$ at different temperature in the range 2–80 K. Measurements performed on IN4C (ILL), at incident energy $E_0 = 36$ meV (energy resolution $\Delta E_0 = 1.75$ meV).

residual oscillation it causes in the quasielastic part of the Yb spectrum around $E = 7.5$ meV (the energy of the lowest Tm^{3+} CF peak), it seems that it cannot account entirely for the observed intensity. Another possible origin could be the existence of mixed excitation modes, in a spectral range where different types of interactions are involved in the excitations probed by neutrons. In any case, the striking result is that the RM peak at 15 meV is essentially suppressed by Tm substitution for such low concentrations as $x_{\text{Tm}} = 0.15$, and even $x_{\text{Tm}} = 0.08$.

Lastly, the spin-gap filling behavior differs depending on Tm concentration. Substituting 8% Tm results in a visible decrease of the temperature at which this process takes places. With 15% Tm, the spectrum changes qualitatively even at the

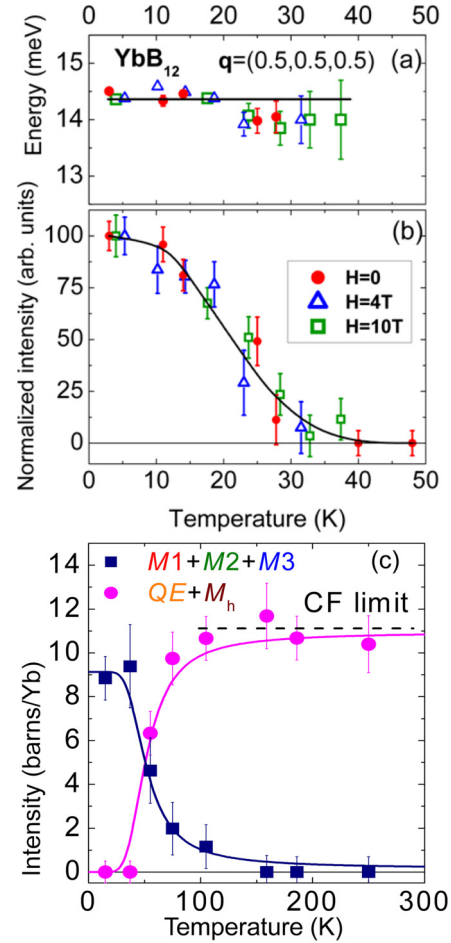


FIG. 7. (Color online) Temperature and magnetic field dependence of the energy (a) and integrated intensity (b) of the spin-exciton RM ($E \sim 15$ meV) in YbB_{12} at the L point in the Brillouin zone, measured on the triple-axis spectrometer IN8 (ILL) in the constant- Q mode (from Ref. [8]). (c) Temperature evolution of the total integrated intensities of the low-temperature spectrum in the gapped state (squares) and of the high-temperature (spin-fluctuations + CF transition) spectrum (closed circles) in YbB_{12} [6,7,15].

lowest temperature, $T_{\text{min}} = 2$ K, the gap is already partly filled, and the filling is almost completed near 40 K.

IV. DISCUSSION

The experimental neutron scattering study performed in IN4C at low energy transfer and with improved energy resolution has revealed (i) the difference in the CF potential of YbB_{12} with respect to those of LuB_{12} and (from the data in Ref. [11]) TmB_{12} , which seem very close to each other, and (ii) the strong influence of the Tm impurities on the magnetic excitation spectrum of Yb in YbB_{12} , affecting its structure as well as its temperature evolution. We will now discuss these two points separately.

A. Thulium as a probe of CF potential in RB_{12}

The Tm magnetic excitation spectra are well described by a standard CF model for a site with cubic point symmetry. The

present data for $x_{\text{Tm}} = 0.08, 0.15,$ and 0.75 are in very good agreement with the CF splitting scheme, with a Γ_5 triplet ground state, suggested in Ref. [11], which corresponds to the set of parameters $W = 0.102$ meV, $X = -0.063$ in Lea, Leask, and Wolff's (LLW) notations [16]. This triplet has strong transition matrix elements with the lower two excited states which are doublet Γ_3 (the strongest) and triplet Γ_4 , at energies of about 7 and 14 meV, and much weaker ones with another triplet Γ_5 and a doublet Γ_2 at higher energies (≈ 21 and 28 meV). At low temperature, the magnetic triplet ground state with a large magnetic moment of about $4.7 \mu_B$ naturally leads to a long-range order in pure TmB_{12} . The large magnetic moment in the CF ground state of Tm^{3+} is also important to understand the effect of Tm impurities substituted on the Yb sublattice in YbB_{12} .

In the present measurements, a remarkable difference in the energies of the Tm CF transitions has been observed between Lu- and Yb-based solid solutions. As noted in Sec. III, the shift amounts to a decrease by approximately 4% in the energy of each excited level ($\Gamma_3, \Gamma_4, \Gamma_5$) for (Yb, Tm) B_{12} in comparison with (Lu, Tm) B_{12} . Considering that the energies of the different levels have different functional dependences on the CF parameter X (see [17]), it can be inferred that the main contribution to the observed variation originates in a decrease of the overall scaling factor W . Using the LLW [16] parametrization

$$\hat{H} = W \left[x \frac{\hat{O}_4}{F(4)} + \{1 - |x|\} \frac{\hat{O}_6}{F(6)} \right]$$

for the CF Hamiltonian in cubic symmetry, the observed positions and relative intensities of the three excitation peaks lead to $x = -0.060$ and $W = 0.1016$ meV for (Lu,Tm) B_{12} , and to $x = -0.060$ and $W = 0.0975$ meV for (Yb,Tm) B_{12} . As expected, the shift in the peak positions is reflected into a reduction of W by about 4%.

The above values of W and x are directly related to the phenomenological fourth and sixth order CF coefficients B_4 and B_6 . Assuming a Coulomb-type functional dependence of the CF potential for small variations of the distance R between the RE ion and the 24 B atoms in the first coordination sphere, we can write $\Delta B_n/B_n = (n+1) \Delta R/R$. Since the relative change $\Delta R/R$ between LuB_{12} and YbB_{12} , derived from structural data [10], is only $\sim 7 \times 10^{-4}$, the resulting change in the CF scale factor W corresponding to this effect should not exceed 0.5%. This value is almost one order of magnitude smaller than obtained experimentally (4%, see above). The main change must therefore come from conduction electron contributions, which can be quite different in the "mixed-valence semiconductor" compound YbB_{12} as compared to its metallic trivalent neighbors TmB_{12} and LuB_{12} .

If one calculates effective point charges for the 24 nearest boron neighbors of Tm from the experimental CF B_n parameters, the values obtained are positive and different for B_4 and B_6 . This unphysical result reinforces the idea that there is indeed a strong contribution from conduction electrons in the actual CF potential of this material. It can be noted that, in RE hexaborides, a similar analysis of the CF data results in *negative* effective charges, which is more consistent with a general treatment of electronic properties in boron-cluster

systems. Under certain conditions,³ the values of B_n can be expressed as the product

$$B_n = \Theta(J)_n \langle r_{4f}^n \rangle A_n,$$

$\Theta(J)_n$ is a so-called Stevens coefficient, which is tabulated for each RE ion (see, for instance, [16]); $\langle r_{4f}^n \rangle$ is related to the radial extension of the $4f$ electron wave function of the ion and can be found in the literature, whereas A_n depends only on the value and spatial distribution of charges around the RE site, thus being directly related to the CF potential from neighbor ions and conduction electrons. The values of A_n associated with the observed splitting of the Tm^{3+} multiplet ($J = 6$) in YbB_{12} or LuB_{12} (neglecting the above-mentioned 4% difference) are $A_4 \approx -9$ meV \AA^{-4} , and $A_6 \approx -29$ meV \AA^{-6} , in good agreement with those derived in Ref. [15] from the CF splitting of Er^{3+} impurities in YbB_{12} ($A_4 \sim -11$ meV \AA^{-4} , and $A_6 \sim -22$ meV \AA^{-6}). If, on the other hand, one tries to estimate the overall CF splitting in Yb^{3+} based on the above results, the predicted value is only $\delta_{\text{CF}} \approx 11$ meV. This is about two times less than the energy of the single broad inelastic peak observed in the "high temperature" ($T > 70$ K) spectra of YbB_{12} , which is thought to reflect CF effects within the incoherent spin-fluctuation regime ($T_{\text{sf}} \sim 100$ K). It thus appears that the hybridization of the Yb f -electron states with conduction electron states in the intermediate valence state of YbB_{12} results not only in a reduction of the effective CF potential acting on the Tm ion impurities but also in a strong increase of the energy splitting of the Yb atoms forming the host lattice.

It is known that the valence mixing can strongly affect the CF potential acting on paramagnetic impurities.⁴ This has been observed, for instance, in neutron experiments on (Ce,Pr) Ni_5 [17], where Ce exhibits a very high degree of f -electron delocalization. Another limiting case is the heavy-fermion compound (Ce,Pr) Al_3 [17,18]. In the latter system the CF splitting of the Ce ions varies by as much as 20% when the heavy-fermion state forms with decreasing temperature, but no significant change occurs in that of paramagnetic Pr impurities.

Therefore, the present case of (Yb,Tm) B_{12} seems closer to that of heavy-fermion systems, but with some incipient f -electron delocalization, which is weak but sufficient to produce a 4% decrease in the CF splitting of the impurity, together with a rather strong (100% instead of 20% in the case of a classical heavy-fermion compound) renormalization of the CF splitting of the "host" atom.

One additional remark can be made in connection with the possibility of a structural distortion in LuB_{12} (and YbB_{12} as well) at temperatures below 80 K, which was suggested in a recent publication [19]. The CF is quite sensitive to such effects, as was shown in a variety of situations (amorphization of RE intermetallics, ionic substitution in solid solutions, etc.). Therefore, a very small lattice distortion occurring in the vicinity of a CF-sensitive ion may have drastic effects,

³In particular there should be no mixing between the f -electron density and the surrounding charge distribution.

⁴In such systems CF transitions are usually observed only for impurities, not for the host rare-earth ions, which are dominated by spin-fluctuation effects.

from a substantial broadening of the transitions to a complete rearrangement of the CF level scheme. In the present experiment we have fitted the CF excitation peaks at all temperatures between 2 and 80 K and found no evidence of a broadening which should be induced by structural disorder supposed in [19] for some part of the sample at low temperature, within the limit of experimental accuracy (10% or less).

B. Magnetic excitation spectra of Yb under the influence of Tm

Let us now focus on the data presented in Fig. 6. The first obvious effect of Tm substitution is the suppression of the spin-exciton RM at 15 meV. From our detailed single-crystal study of YbB₁₂, it was demonstrated that this mode exists as a narrow peak in the spectra possessing a well-formed spin gap. In Fig. 6(a) it is clearly seen that the RM disappears *before* the gap starts to fill as temperature increases. From our previous studies, the RM excitation is known to exhibit energy dispersion and a modulation of its intensity within the Brillouin zone, which is characteristic of cooperative excitations from the Yb singlet ground state. In the case of isoelectronic substitution by nonmagnetic Lu³⁺ ions [15], the exciton peak broadens but remains observable up to a concentration of $x_{\text{Lu}} = 0.25$. The present data show that the introduction of isoelectronic *magnetic* defects (Tm³⁺ triplet ground state with a magnetic moment of 4.7 μ_B) suppresses the RM peak at a much lower concentration (no more than $x_{\text{Tm}} = 0.08$). This indicates that defects carrying a magnetic moment (the moment in the CF ground state of Yb³⁺ in the YbB₁₂ host is estimated to be $\approx 2.2 \mu_B$) destroy the coherent spin excitations more effectively than nonmagnetic ones. The mechanism of this effect may be seen as twofold not only do the stable-valence 4*f* shells at the Tm³⁺ sites lack the capability of contributing to the coherent hybridized state, but their net magnetic moments also act as effective scatterers for the quasiparticles.

The spin-exciton RM appears as the weakest component of the magnetic excitation spectra with respect to the different types of disorder, and is most strongly affected by extra Tm³⁺ magnetic moments. The latter observation is consistent with the initial idea of [20] that the exchange interaction is the driving force stabilizing this mode within the gap.

The second effect of Tm substitution is to gradually destabilize the spin gap. Initially ($x_{\text{Tm}} = 0$ to 0.08) the temperature of the transition from the gap state to the spin-fluctuation regime goes down. Further increasing the concentration ($x_{\text{Tm}} = 0.15$) results in the replacement of the gap by a pseudogap down to the lowest temperature of the measurements ($T_{\text{min}} = 2$ K). This is illustrated in Fig. 8, which presents selected spectra for Yb_{1-x}Tm_xB₁₂ ($x_{\text{Tm}} = 0, 0.08, 0.15$) at $T = 2$ K [Figs. 8(a), 8(c), and 8(d)], and for pure YbB₁₂ at $T = 80$ K [Fig. 8(b)]. The inelastic part of the data for $T = 2$ K can be fitted using two inelastic peaks (plus the RM peak for $x_{\text{Tm}} = 0$). At $T = 80$ K the YbB₁₂ spectrum exhibits a clear Lorentzian quasielastic component, together with a single inelastic peak, in accordance with our previous measurements [6]. For $x_{\text{Tm}} = 0.15$, the quasielastic component still exists at $T = 2$ K [Fig. 8(d)].

The main difference between the spectra for $x_{\text{Tm}} = 0.08$ and 0.15 at $T_{\text{min}} = 2$ K thus turns out to be the partial filling of the gap at the higher Tm concentration. This can be seen

in Fig. 8(e), where the two data sets could practically be superimposed, within the limits of error bars, after subtracting out the residual quasielastic signal, represented by a Lorentzian line shape, from the $x_{\text{Tm}} = 0.15$ spectrum.

The evolution of the quasielastic signal is summarized in Fig. 9. The data points shown in this plot represent the integrated intensity of the quasielastic Lorentzian line shape used for fitting the spectral response in the spin-fluctuation regime [see, for example, Figs. 8(b) and 8(d)], when the suppression of the singlet ground state restores a magnetic density of states within the gap. This approach was used in previous work to represent the temperature evolution of the magnetic excitation spectrum in pure YbB₁₂ and in Lu-substituted solid solutions. In the (Yb,Tm)B₁₂ series, the half-width of quasielastic signal $\Gamma_{\text{sf}}/2$ stayed close to the value determined for YbB₁₂ [21], on the order of 9 to 11 meV. This value represents the spin-fluctuation energy $E_{\text{sf}} = k_B T_{\text{sf}}$ of the system.

The influence of a low concentration of Tm ions on the Yb magnetic excitation spectrum is rather strong in comparison to that previously reported for other types of YbB₁₂-based solid solutions [15,21,22]. Only in the case of Zr [22] was the effect comparable in magnitude (20% of nonmagnetic Zr comparable to 15% of Tm). In that case, however, the temperature evolution became slower in comparison with YbB₁₂, and the spin-gap suppression process extended to rather high temperatures, whereas Tm substitution results in the spin gap being suppressed at lower temperature than in pure YbB₁₂. With isoelectronic Lu substitution, which can be viewed as a mere dilution of Yb magnetic moments, the gap was not significantly reduced up to more than 50% Lu concentration [23]. We also recall that the application of an external magnetic field of up to 10 T (Fig. 7) produced no significant change either in the properties of the RM or in the temperature evolution of the spin gap [8].

The narrow in-gap mode found in YbB₁₂ was initially interpreted within Riseborough's simple spin-exciton picture [20]. Subsequent theoretical work focused on YbB₁₂ considered additional effects from the crystal field [24], or from interactions between rare-earth ions [25]. The observation of a strong effect on the RM of isoelectronic magnetic impurities (Tm³⁺) provides incentives for developing more realistic models.

Even before the beginning of our work on YbB₁₂, a sharp low-energy excitation had been identified in the well-known mixed-valence system SmB₆ [26]. This compound is currently undergoing a strong revival of interest as a possible example of a "topological insulator." A detailed inelastic neutron scattering study of that excitation in isotopically enriched, single-crystal SmB₆ and its solid solutions documented its dependence on the momentum transfer and the Sm valence state [26,27]. These experiments were recently revisited in the light of our work on YbB₁₂ [8]. As in the latter compound, the excitation can be interpreted as an in-gap resonance mode, associated with the spin gap forming at low temperature in the KI regime. However, the physical origin may differ between the two systems [8]. Further understanding of the RM in SmB₆ could likely be gained by studying the effect of magnetic impurity substitution, as was done in the present study for YbB₁₂.

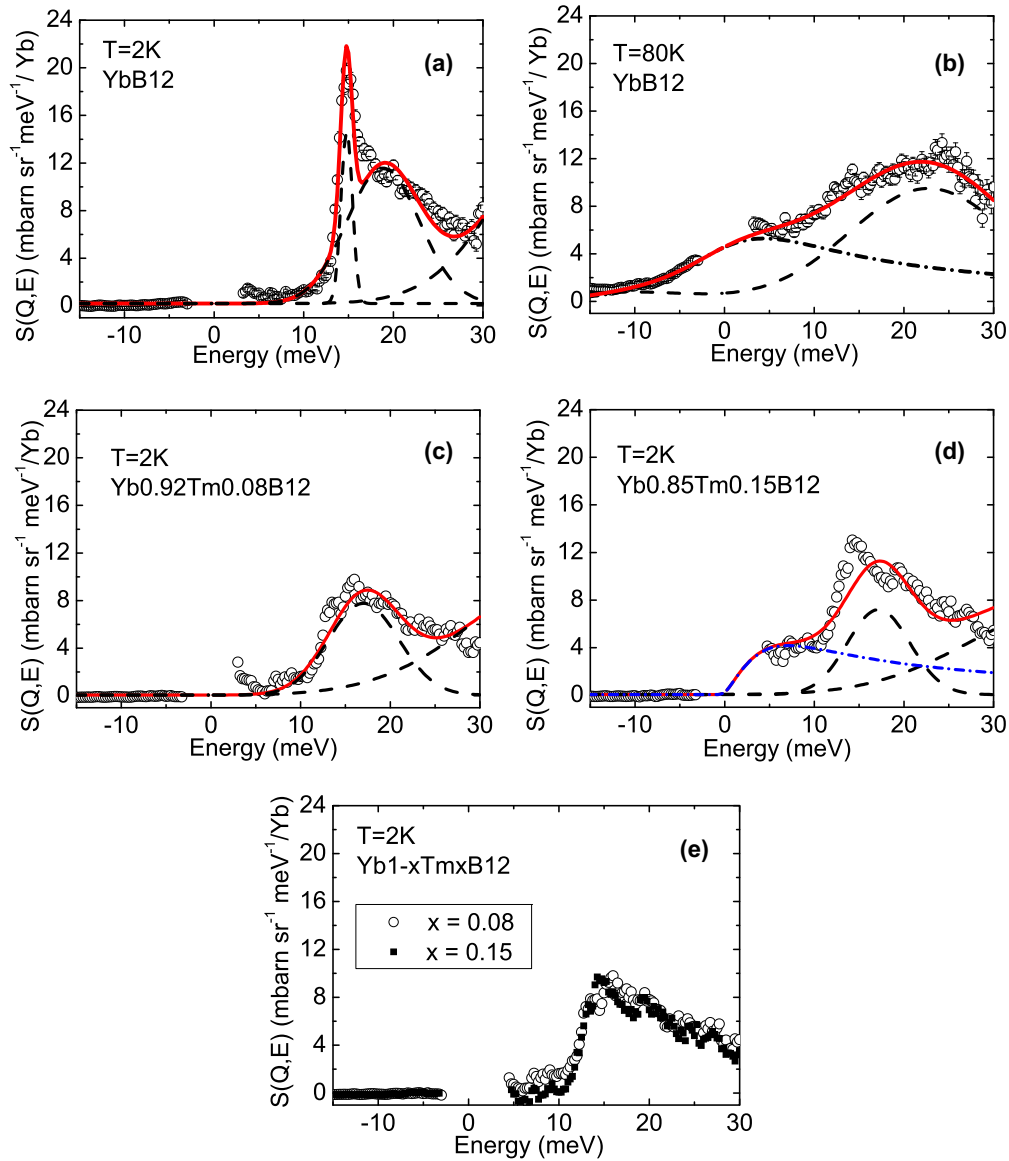


FIG. 8. (Color online) Magnetic scattering spectra for YbB_{12} at $T = 2$ K (a) and 80 K (b), and for $\text{Yb}_{1-x}\text{Tm}_x\text{B}_{12}$ (Tm contribution subtracted) at $T = 2$ K [$x = 0.08$ (c) and $x = 0.15$ (d)]. The dash-dotted line in frames (b) and (d) corresponds to a fit of the spin-fluctuation contribution by a quasielastic Lorentzian line shape (half-width $\Gamma_{\text{qe}} \sim 9$ meV), taking into account the detailed balance factor. The dashed lines represent the decomposition of the inelastic magnetic signal into different contributions according to our previous interpretation of the magnetic response in YbB_{12} [6,7], namely one narrow peak at 15 meV and two broad peaks at 20 and 40 meV at low temperature, and one single broad peak at about 25 meV at high temperature. (e) Compares the result obtained by subtracting a spin-fluctuation contribution associated with the in-gap density of states (represented by a quasielastic Lorentzian spectral function) from the experimental pseudogap spectrum of $\text{Yb}_{0.85}\text{Tm}_{0.15}\text{B}_{12}$ (closed squares) to the as-measured spectrum for $\text{Yb}_{0.92}\text{Tm}_{0.08}\text{B}_{12}$ (open circles).

To understand how such dramatic changes can occur over a narrow range of Tm concentrations, one can refer to a recent study [28] of another strongly correlated insulator FeSi, belonging to the family of transition metal silicides TSi ($T = \text{Fe, Mn, Co}$). The substitution of Mn for Fe corresponds to the introduction of magnetic ions on the d -element sublattice (contrary to FeSi, MnSi exhibits long-range helimagnetic order at low temperature). It was found that a few percent of Mn change the physical (magnetic and transport) properties drastically. In Ref. [28] this was taken to demonstrate the possibility of achieving a non-Fermi-liquid behavior through the so-called “under-compensated Kondo effect,” in which there are too

few mobile electrons to compensate the spin of unpaired electrons localized on impurity atoms. Similarly, in case of Tm impurities introduced on the Yb sublattice of YbB_{12} , the Tm^{3+} magnetic moments can remain uncompensated, even at low temperature, causing inelastic scattering of the electronic carriers, while disrupting the coherent character of the ground state intrinsically connected to band electrons.

The extra scattering channels for charge carriers, along with the changes produced in the magnetic excitation spectrum, can have drastic effects on the thermoelectric properties of $\text{Yb}_{1-x}\text{Tm}_x\text{B}_{12}$. It was shown recently, in an extensive review article [29], that CF splitting and Kondo effect could contribute

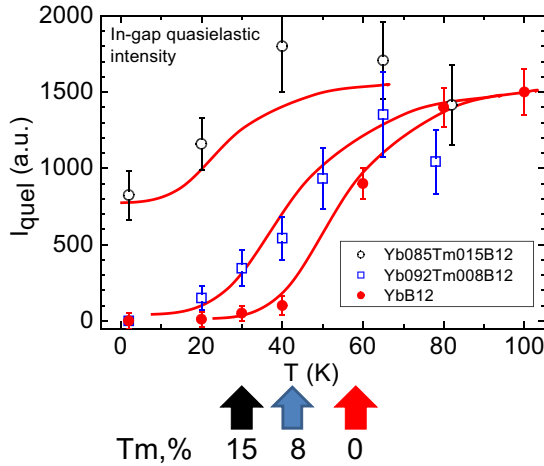


FIG. 9. (Color online) Temperature dependence of the intensity (I_{quel}) of the signal gradually filling the spin gap, for $\text{Yb}_{1-x}\text{Tm}_x\text{B}_{12}$ with $x = 0$ (closed circles), 0.08 (squares), and 0.15 (open circles). Intensities were normalized to 1 g at. of Yb. Arrows approximately denote the temperature at which half-filling of the gap is reached upon heating.

to the thermopower in different temperature ranges for Kondo systems. Assuming Δ_{CF} to be much larger (up to an order of magnitude) than the Kondo temperature T_{K} , two peaks can be observed in the temperature dependence of the thermoelectric coefficient a maximum, due to the CF contribution, at a temperature T_1 which is comparable to, or somewhat smaller than Δ_{CF} , and a second peak at about $T_2 \sim T_{\text{K}}/2$, i.e., far below Δ_{CF} .

In YbB_{12} , T_1 and T_2 can be roughly estimated, from the neutron scattering data, to be about $T_1 \sim 100\text{--}200$ K ($\Delta_{\text{CF}} \sim 230$ K) and $T_2 \sim 40\text{--}50$ K ($T_{\text{K}}, T_{\text{sf}} \sim 100$ K). As can be seen in Fig. 1, three notable features are present in the temperature dependence of the Seebeck coefficient $S(T)$ (i) one shoulder close to, or slightly above, 100 K, (ii) a peak at about 30–40 K, and (iii) another peak at 10 K. The first two are in qualitative agreement with the above estimates of T_1 and T_2 . The third one appears to be less stable against Tm and, to some extent, Lu substitution, and could be related to the formation of the spin-exciton state responsible for the RM, which fully develops only below 30 K.

As shown above, increasing the Tm impurity concentration first suppresses the RM in the neutron spectrum. Accordingly, the feature in the TEP ascribed to the T_{sf} energy scale and the spin-gap opening can expand with decreasing temperature, without interference from the RM (in-gap) mode formation. This effect is seen in Fig. 1, for $0 < x_{\text{Tm}} \leq 0.2$, as the suppression of peak (iii), together with a dramatic

enhancement of peak (ii). At larger Tm concentrations ($x_{\text{Tm}} > 0.2$), hybridization effects and, consequently, the spin gap itself, are gradually suppressed, resulting in a fast decrease in the amplitude of peak (ii). Finally, only a broad negative minimum, likely related to the CF splitting of Yb, survives in the Tm-rich compounds ($x_{\text{Tm}} = 0.5\text{--}0.7$) in the vicinity of the insulator-metal transition in $(\text{Yb},\text{Tm})\text{B}_{12}$ (closing of the conductivity gap).

These considerations on a possible relationship between the magnetic excitation spectra and the temperature dependence of the Seebeck coefficient are only qualitative. No detailed theoretical model is currently available. We simply wanted to point out the intriguing correspondence between the effect of Tm and Lu impurities on the TEP, on the one hand, and on magnetic excitation spectra, on the other hand.

V. CONCLUSION

The effect of isoelectronic substitution of magnetic Tm^{3+} on the energy structure and temperature dependence of the dynamical magnetic response in $\text{Yb}_{1-x}\text{Tm}_x\text{B}_{12}$ solid solutions has been studied using inelastic neutron scattering. The spin-exciton-like resonance mode near 15 meV is steeply suppressed at the lowest measured Tm concentration of $x_{\text{Tm}} = 0.08$. The spin gap is replaced by a pseudogap at concentrations lower than 0.15. This is thought to reflect the presence of magnetic moments on Tm ions, even at the lowest temperature, because of their triplet CF ground state. The introduction of extra scattering centers for the band electrons results in a loss of coherence causing a modification, then the complete suppression, of the gapped excitation spectrum characteristic of the Kondo-insulator ground state in pure YbB_{12} . This effect bears interesting similarities to the “undercompensated Kondo effect” invoked to explain the influence of magnetic impurities in another well-known strongly correlated insulator FeSi. A correspondence was suggested between the concentration dependence of the magnetic response observed in this work and that of the TEP coefficient $S(T)$.

It was also found that the CF potential is different in YbB_{12} from that in LuB_{12} and in TmB_{12} . A plausible explanation is a change in the contribution of conduction electrons to the CF potential due to mixed-valence state of Yb, associated with a significant hybridization between localized $4f$ and conduction-band electrons.

ACKNOWLEDGMENT

We acknowledge financial support from the RFBR Grants No. 12-02-12077 and No. 14-02-00272. Discussions with N. E. Sluchanko, V. V. Glushkov, and experimental support of T. Guidi are strongly appreciated.

- [1] F. J. Di Salvo, *Science* **285**, 703 (1999).
- [2] N. E. Sluchanko, A. V. Bogach, V. V. Glushkov *et al.*, *JETP Lett.* **89**, 256 (2009).
- [3] F. Iga, T. Suemitsu, S. Hiura *et al.*, *J. Magn. Magn. Mater.* **226-230**, 137 (2001).

- [4] J. M. Mignot, P. A. Alekseev, K. S. Nemkovski, L. P. Regnault, F. Iga, and T. Takabatake, *Phys. Rev. Lett.* **94**, 247204 (2005).
- [5] H. Okamura, S. Kimura, H. Shinozaki, T. Nanba, F. Iga, N. Shimizu, and T. Takabatake, *Phys. Rev. B* **58**, R7496(R) (1998).

- [6] E. V. Nefeodova, P. A. Alekseev, J.-M. Mignot, V. N. Lazukov, I. P. Sadikov, Y. B. Paderno, N. Y. Shitsevalova, and R. S. Eccleston, *Phys. Rev. B* **60**, 13507 (1999).
- [7] K. S. Nemkovski, J. M. Mignot, P. A. Alekseev, A. S. Ivanov, E. V. Nefeodova, A. V. Rybina, L. P. Regnault, F. Iga, and T. Takabatake, *Phys. Rev. Lett.* **99**, 137204 (2007).
- [8] K. S. Nemkovski, P. A. Alekseev, J.-M. Mignot, and A. S. Ivanov, *Phys. Proc.* **42**, 18 (2013).
- [9] N. E. Sluchanko, A. N. Azarevich, A. V. Bogach, V. V. Glushkov, S. V. Demishev, M. A. Anisimov, A. V. Levchenko, V. B. Filipov, and N. Yu. Shitsevalova, *JETP* **115**, 509 (2012).
- [10] H. Werheit, V. Filipov, K. Shirai *et al.*, *J. Phys. Condens. Matter* **23**, 065403 (2011).
- [11] A. Murasik, E. Clementyev, and A. Czopnik, Report IAE - 99/A, (2003) Świerk, Poland.
- [12] K. S. Nemkovski, J.-M. Mignot, and R. I. Bewley, ISIS Experimental Report RB920234.
- [13] A. P. Murani, *Phys. Rev. B* **50**, 9882 (1994).
- [14] A. V. Rybina, P. A. Alekseev, J.-M. Mignot *et al.*, *J. Phys. Conf. Series* **92**, 012074 (2007).
- [15] P. A. Alekseev, J.-M. Mignot, and K. S. Nemkovski, *J. Phys. Condens. Matter* **16**, 2631 (2004).
- [16] K. R. Lea, J. M. Leask, and W. P. Wolf, *J. Phys. Chem. Solids* **23**, 1381 (1962).
- [17] P. A. Alekseev, V. N. Lazukov, and I. P. Sadikov, *J. Magn. Magn. Mater.* **76-77**, 423 (1988).
- [18] P. A. Alekseev, W. Buehrer, V. N. Lazukov, E. V. Nefeodova, I. P. Sadikov, and O. D. Chistyakov, *Physica B* **217**, 241 (1996).
- [19] N. E. Sluchanko, A. N. Azarevich, A. V. Bogach *et al.*, *JETP* **113**, 468 (2011).
- [20] P. S. Riseborough, *J. Magn. Magn. Mater.* **226-230**, 127 (2001).
- [21] P. A. Alekseev, E. V. Nefeodova, U. Staub *et al.*, *Phys. Rev. B* **63**, 064411 (2001).
- [22] K. S. Nemkovski, P. A. Alekseev, J.-M. Mignot, E. A. Goremychkin, A. A. Nikonov, O. E. Parfenov, V. N. Lazukov, N. Y. Shitsevalova, and A. V. Dukhnenko, *Phys. Rev. B* **81**, 125108 (2010).
- [23] K. S. Nemkovski, P. A. Alekseev, J.-M. Mignot, and V. N. Lazukov, *Phys. Solid State* **52**, 936 (2010).
- [24] A. Akbari, P. Thalmeier, and P. Fulde, *Phys. Rev. Lett.* **102**, 106402 (2009).
- [25] A. F. Barabanov and L. A. Maksimov, *Phys. Lett. A* **373**, 1787 (2009).
- [26] P. A. Alekseev, J.-M. Mignot, J. Rossat-Mignod *et al.*, *J. Phys. Condens. Matter* **7**, 289 (1995).
- [27] P. A. Alekseev, J.-M. Mignot, V. N. Lazukov *et al.*, *J. Solid State Chem.* **133**, 230 (1997).
- [28] N. Mayala, J. F. DiTusa, G. Aeppli, and A. P. Ramirez, *Nat. Lett.* **454**, 976 (2008).
- [29] B. Coqblin, B. Chevalier, and V. Zlatic, in *Properties and Applications of Thermoelectric Materials*, edited by V. Zlatic and A. C. Hewson, NATO Science for Peace and Security Series B (Springer, New York, 2009), p. 91.